Geometrical model of a self-propelled broken interface

Miki Y. Matsuo and Masaki Sano

Department of Physics, The University of Tokyo - Hongo, Bunkyo-ku, Tokyo, Japan

E-mail: miki@daisy.phys.s.u-tokyo.ac.jp

Abstract. We consider a geometrical model of a broken interface showing self-propelling motion. This model is constructed to comprise a static solution with a spontaneous curvature. Furthermore, by introducing a nonlocal interaction force into the geometrical model, we show that the static solution causes spontaneous drift motion even when the nonlocal force is infinitesimal. This drift motion appears via transcritical bifurcation.

PACS numbers: 05.70.Np, 47.54.-r

Submitted to: *J. Phys. A: Math. Gen.*

1. Introduction

The dynamics of a self-propelled object is a fundamental problem in nonequilibrium physics. Recent experiments have several examples of self-propelled objects. Bimetallic rods [1], sphere-dimer motors [2, 3], and Janus particles [4, 5] driven physically or chemically are examples of self-propelled dynamics whose persistent self-propelled motion is due to the broken symmetry implemented in their materials. There are also various systems in which the broken symmetry is self-organized, such as self-propelled oil droplets in water containing surfactant molecules [6] or self-propelled motions of vesicles in which chemical reactions occur [7]. The localized pattern in reaction-diffusion systems, called "spots," is also an example of a self-propelled object [9, 8]. The spot pattern shows self-propelling motion in semiconductor materials, gas discharge phenomena [10], and chemical systems [11]. Thus, we recognize many phenomena that demonstrate self-propelling dynamics.

Except for asymmetry-implemented solid materials, many self-propelled objects are soft and wet materials, which more or less accommodate the deformation of their shapes through the self-propelling motion. A self-propelled oil droplet shows large deformation when the surfactant gradient and the resultant velocity are large [6]. Spot motion numerically investigated by Krischer *et al.* shows that a spot changes its shape as the propagating velocity increases [8]. Thus, we know various self-propelling soft materials, and, however, we do not clearly know how the deformation of the material is influential in these phenomena. It might be considered that the deformation is simply an extrinsic phenomenon accompanying centroid motion; however, the counteraction of motion induced by asymmetry in shape cannot be excluded. There might be even a case that the pure geometric effect of deformation can induce the motion of matter. It must be noted that, in these previous studies, the effects of a geometric component and the other internal degrees of freedom such as activator-inhibitor concentration, surfactant gradient, temperature gradient, and pressure gradient are not clearly distinguished.

Thus, in this letter, we clarify the relationship between a purely geometric effect of the interface and the self-propelled motion. If our theory can not reproduce some property of self-propelling motion, we can conclude that the property is not coming from the geometric effect but other important properties. We consider an open interface having two free terminals with conserved arclength rather than a closed circular interface, because the closing condition makes the problem more complicated. The study of a purely geometric component of interface dynamics was first considered by Brower *et al.* [12]; they introduced a geometrical model whose dynamics is determined by local equations at the surface. Here, "local" implies that the velocity is locally determined by the curvature and its derivative. This is a drastic hypothesis because the motion of the interface is an extremely complex function of the interfacial position in general interface growth dynamics. For example, in the case of spot motion in reaction-diffusion systems, the complete motion might require the solution of a partial-differential equation throughout the entire d-dimensional space. Nevertheless, Brower

et al. clarified that some features of the motion are followed by the kinematics of a locality assumption [12]. Thus, with help of Brower's description, we examine whether only geometric constraints can cause self-propelled motion. Within this framework, we will conclude that the geometrical model can describe the occurrence of self-propelled motion, while the breakdown of locality must be assumed.

2. Motion by local interface growth

Here, we consider the description of one-dimensional interfacial surface with local interface growth in a two-dimensional space. The interfacial surface specified by the position vector $\mathbf{r}$ is assumed to be governed by the instantaneous time-evolving equation

$$\frac{d\mathbf{r}}{dt} = \hat{L}_0\mathbf{r}. \tag{1}$$

The nonlinear operator $\hat{L}_0$ is generally described by

$$\hat{L}_0\mathbf{r} = U\mathbf{n} + V\mathbf{t} \tag{2}$$

in two-dimensional space, where $\mathbf{n}$ and $\mathbf{t}$ are the normal and tangent vectors, respectively, and U and V are the associated forces. In general interface growth dynamics, the operator $\hat{L}_0$ can have an extremely complex functional form of the interfacial position. Here, we use the locality assumption in which $\hat{L}_0$ includes only the local quantity of interface position. That is, U and V are the functionals of $\mathbf{r}$ and its derivatives: $U \simeq U(\mathbf{r}, \nabla\mathbf{r}, \cdots)$. Equation (1) must be gauge invariant implying that we can arbitrarily use the extrinsic coordinate α as a parametrization. Here, we specifically select the parameter $-\pi \leq \alpha \leq \pi$ satisfying $\dot{\alpha} = 0$ as an extrinsic representation. This parametrization is called orthogonal gauge by Brower *et al.* [12]. On the other hand, it is advisable to use a gauge invariant intrinsic coordinate s for the description of the equation in which the normal and tangent vectors become unit vectors. The Frenet-Serret formula $\mathbf{r}_s = \mathbf{t}, \mathbf{t}_s = -\kappa\mathbf{n}$, and $\mathbf{n}_s = \kappa\mathbf{t}$ are applied for the relationship among between $\mathbf{r}, \mathbf{t}$, and $\mathbf{n}$, where κ is the local curvature of the interface. The metric g is defined by $\sqrt{g} \equiv \partial s/\partial\alpha$, and the arclength s is given by $s(\alpha) = \int^{\alpha} \sqrt{g} d\alpha'$.

In this letter, we consider a broken interface having spontaneous curvature and two free terminals. In order to append the spontaneous curvature into the model, we assume the phenomenological relation

$$U = 1 - \kappa, \tag{3}$$

where κ is the curvature. The other simple phenomenological relation $U \sim -\kappa$ is discussed later. V is treated as a multiplier to preserve the arclength under the boundary condition $V = 0$ at $s = -\pi, \pi$. Note that both of U and V are nonequilibrium active forces, which is not determined by a variational principle. When we consider an equilibrium system such as a stiff polymer, the multiplier satisfying the arclength preservation is not determined by only V but also U, in which the multiplier is a local surface tension $\Lambda(\alpha)$ defined by the energy constraint $\mathcal{H} = \int \sqrt{g}\Lambda(\alpha)d\alpha$. The

variation of the free energy gives $U = -\Lambda\kappa$ and $V = \Lambda_s$ [13]. However, assuming general nonequilibrium cases, we independently determine each force in this paper.

Equations (1) and (3) have a trivial stable uniform solution with $\kappa = 1$. When the interface is specified by $-\pi < s \leq \pi$, the trivial solution is given by

$$\mathbf{r} = \mathbf{r}(0) + \int_0^s ds e^{i(s+\theta_0)}, \tag{4}$$

where θ_0 is the phase of the origin. We used the conventional notation for vector and complex number describing the curve by the complex position $\mathbf{r} = x + iy$. In this letter, we continue to use this notation for the description of vectors. Hereafter, we investigate the dynamics in the vicinity of the trivial solution.

Now, we analyze Eq. (1). Using the phase θ defined by $\kappa = \theta_s$, we rewrite Eq. (1) as

$$\dot{\theta} = -U_s + \kappa V, \tag{5}$$

$$\dot{g} = 2\kappa g U + 2g V_s. \tag{6}$$

The phase equation is rewritten as

$$\frac{\partial\theta}{\partial t} = -\frac{\partial}{\partial s}U + \kappa V - \frac{\partial\theta}{\partial s}\int^s \{\kappa U + V_s\} ds. \tag{7}$$

We request that the metric is invariant over the time-evolution, which is necessary to preserve the arclength. Using this requirement, we determine the tangential force V by

$$V_s = -\kappa U. \tag{8}$$

Using the boundary condition $V = 0$ at $s = -\pi, \pi$ and the reflection symmetry around $s = 0$, we can confirm that the integration constant in Eq. (8) is zero. Under these conditions, we finally obtain the phase equation

$$\frac{\partial\theta}{\partial t} = -\frac{\partial}{\partial s}U - \frac{\partial\theta}{\partial s}\int^s \theta_s U ds, \tag{9}$$

which is identically described using the curvature by

$$\frac{\partial\kappa}{\partial t} = -\left(\kappa^2 + \frac{\partial^2}{\partial s^2}\right)U - \frac{\partial\kappa}{\partial s}\int^s \kappa U ds. \tag{10}$$

Although we can equivalently use either description (9) or (10) for further analysis, we prefer to use the phase equation (9). Introducing Eq. (3) into Eq. (9), we get

$$\partial_t\phi = \phi_{ss} + (1+\phi_s)\int^s (1+\phi_s)\phi_s ds, \tag{11}$$

where the variable ϕ is defined by $\theta = s + \phi + \theta_0$, which implies phase deviation from the precise circular phase. We now perform the linear stability analysis around the uniform solution $\phi = 0$. Ignoring all the nonlinear terms, we obtain the linearized phase equation as

$$\partial_t\phi = \phi_{ss} + \phi. \tag{12}$$

Assuming the reflection symmetry along $s = 0$, we expand with Fourier modes as $\phi = -\sum a_n(t)\sin(ns)$. Thus we get

$$\dot{a}_n = (1 - n^2)a_n. \tag{13}$$

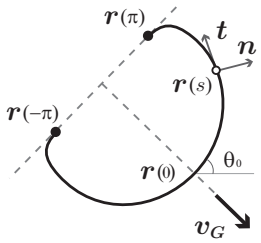

Figure 1. Motion of broken interface. The interface moves to the direction perpendicular to the line connected between the terminal points.

Note that the $n = 1$ mode has a zero eigenvalue. The neutral stability of mode $n = 1$ is discussed later.

Next, we consider the centroid of the interface. When the interface is assumed to be intrinsically uniform, the centroid is described by

$$\mathbf{r}_G = \int_{-\pi}^{\pi} \mathbf{r} ds. \tag{14}$$

Differentiating with t on both-sides of the equation, we get

$$\boldsymbol{v}_G = \int_{-\pi}^{\pi} \hat{L}_0 \mathbf{r} ds, \tag{15}$$

where $\dot{g} = 0$ is used. Hence the centroid velocity becomes

$$\boldsymbol{v}_G = \boldsymbol{v}_G^{(n)} + \boldsymbol{v}_G^{(t)}, \tag{16}$$

where the normal and tangent components are distinguished as

$$\boldsymbol{v}_G^{(n)} = \int_{-\pi}^{\pi} U \mathbf{n} ds, \tag{17}$$

$$\boldsymbol{v}_G^{(t)} = \int_{-\pi}^{\pi} V \mathbf{t} ds. \tag{18}$$

Introducing Eq. (3) into Eq. (17), we get

$$\boldsymbol{v}_G^{(n)} = -i\{\mathbf{r}(\pi) - \mathbf{r}(-\pi)\} + \{\mathbf{t}(\pi) - \mathbf{t}(-\pi)\}. \tag{19}$$

Thus, when Eq. (3) is considered, the normal component of the centroid velocity is quite easily determined by its geometric nature; it is determined by the position and tangent vectors of the two terminals. On the other hand, it is comparatively difficult to further simplify Eq. (18) without any approximation.

To understand the relationship between centroid motion and shape, we assume that some applied perturbation imparted the deformation including only the first Fourier mode to the trivial solution; $\theta = s - a_1 \sin s + \theta_0$. In this case, clearly, $\mathbf{t}(\pi) = \mathbf{t}(-\pi)$ holds. We now calculate the distance between the terminal points, $\Delta\mathbf{r} = \mathbf{r}(\pi) - \mathbf{r}(-\pi)$. Using the formula for a Bessel function

$$\int_0^{2\pi} ds e^{i(ns \pm z \cos s)} = 2\pi i^{\pm n} J_n(z), \tag{20}$$

we get the terminal distance by

$$\Delta\mathbf{r} = 2\pi J_1(a_1) e^{i\theta_0}. \tag{21}$$

In particular, when a_1 is sufficiently small, the relation is approximated by

$$\Delta \mathbf{r} \sim \pi a_1 e^{i\theta_0}. \tag{22}$$

Thus the mode $n = 1$ is strictly related to the distance between the terminal points. Equations (17) and (22) give

$$\boldsymbol{v}_G^{(n)} = -\pi i a_1 e^{i\theta_0} + \mathcal{O}(a_1^2). \tag{23}$$

Next, we estimate the tangential component of the centroid velocity using first order approximation. From Eqs. (3) and (8), V is described by $V_s = -\kappa(1-\kappa)$. Here, we assume that deviation from the trivial static solution $\delta\kappa = \kappa - 1$ is small. Ignoring the $\mathcal{O}(\delta\kappa^2)$ term in V_s, we get $V_s \simeq -(1-\kappa)$. We now consider the case in which $\delta\kappa$ includes only the first Fourier mode, $V_s = -a_1 \cos s$, where sine functions are not included by the symmetry. Then, $V = -a_1 \sin s$ with the assumption that the tangential force is zero at $s = -\pi, \pi$. Using this relationship and Eq. (18), the tangential component of the centroid velocity is given by

$$\boldsymbol{v}_G^{(t)} = -\pi i a_1 e^{i\theta_0} + \mathcal{O}(a_1^2). \tag{24}$$

Equations (23) and (24) are almost similar, and thus the total centroid velocity is given by

$$\boldsymbol{v}_G = -2\pi i a_1 e^{i\theta_0} + \mathcal{O}(a_1^2). \tag{25}$$

Thus, we obtained two fundamental equations (13) and (25) from which we understand several facts applicable to the geometrical model with the locality assumption. Equation (13) shows that the locality assumption always derives the neutral stability of $n = 1$ mode of deformation. With Eq. (25), this fact further implies that the locality assumption gives the neutral stability of the centroid motion. This means that the property of the solution is qualitatively changed by an arbitrary small perturbation, which breaks the symmetry. For example, even when we consider the static solution of the interface, the solution might start to self-propel under the noisy circumstances. To understand the robust and universal description of the interface, we should perform singular perturbation to unfold this singular point [14], which is discussed in the next section.

Lastly in this section, we give a brief remark about the description of a closed curve. If a closed curve is considered, we must further specify the two constraint equations, $\oint \kappa ds = 2\pi$ and $\mathbf{r}(\pi) = \mathbf{r}(-\pi)$. The second constraint is crucial to the motion of a centroid, because Eq. (19) implies that the closing constraint prohibits the creation of the steady centroid motion from normal force. In this case, the tangential force has a significant impact on the motion, which is related to the Marangoni effect [6].

3. Motion by weak, nonlocal interface growth

The locality assumption imparts simplicity to the interface dynamics, but at the same times, it restricts the possible variety of interface dynamics. Here, we relax the

restriction for locality and assume that the breakdown of locality is sufficiently weak so as to be treated as a perturbation. We consider the dynamics of interface

$$\frac{d\mathbf{r}}{dt} = \hat{L}_0\mathbf{r} + \epsilon\hat{L}\mathbf{r}, \tag{26}$$

where $\hat{L}$ is a nonlocal perturbation operator that need not satisfy the locality assumption.

Our aim is to obtain a simple perturbation to break the neutral stability. Here, we show one possible candidate of the simple perturbation. The protocol for the nonlocal perturbation is based on two hypotheses; the first one is called "the locality retrieval condition" which means that the locality is maintained by at least one point on the curve. We assume that the locality is recovered at the origin $s = 0$, hence the operator becomes zero at the recovery point, $\hat{L}\mathbf{r}(0) = 0$. The second hypothesis is that the interface interacts with some virtual interface satisfying the locality retrieval condition. For the virtual interface, we especially consider a precise circle $\mathbf{r}_0$ whose arclength and phase at the origin are identical to the neutrally stable closed interface. The perturbation term $\hat{L}\mathbf{r}$ is assumed to impart harmonic interaction between the broken interface and the virtual interface. From these conditions, $\hat{L}\mathbf{r}$ is determined as

$$\hat{L}\mathbf{r} = \mathbf{r} - \mathbf{r}_0, \tag{27}$$

where

$$\mathbf{r}_0(s) = \mathbf{r}(0) + \int_0^s ds e^{i(s+\theta_0)}. \tag{28}$$

With this nonlocal perturbation, the dynamics of interface are given by

$$\dot{\mathbf{r}} = \hat{L}_0\mathbf{r} + \epsilon\int_0^s e^{i(s+\theta_0)}(e^{i\phi(s)} - 1)ds. \tag{29}$$

The nonlocal force is attractive or repulsive for the cases $\epsilon < 0$ and $\epsilon > 0$, respectively. This equation is rewritten using phase and metric equations such as

$$\dot{\theta} = \hat{L}_0\theta + \epsilon\sin\phi, \tag{30}$$

$$\dot{g} = \hat{L}_0 g + \epsilon 2g(1 - \cos\phi), \tag{31}$$

here $\hat{L}_0\theta$ and $\hat{L}_0 g$ mean the right-hand-sides of Eqs. (5) and (6), respectively. Note that the nonlocal perturbation adds $\epsilon\sin\phi$ term to the phase equation. This term has a significant role in the centroid motion of interface because it gives the linear $\epsilon\phi$ term with the lowest order of expansion, which breaks the neutral stability of the $n = 1$ mode. Assuming that the metric is invariant, we get

$$\begin{aligned}\frac{\partial\theta}{\partial t} = &-\frac{\partial}{\partial s}U - \frac{\partial\theta}{\partial s}\int^s \theta_s U ds \\ &+ \epsilon\sin\phi - \epsilon\frac{\partial\theta}{\partial s}\int^s (1 - \cos\phi)ds.\end{aligned} \tag{32}$$

We introduce Eq. (3) and rewrite it with ϕ, hence we get

$$\begin{aligned}\frac{\partial\phi}{\partial t} = &\phi_{ss} + (1 + \phi_s)\int^s (1 + \phi_s)\phi_s ds \\ &+ \epsilon\sin\phi - \epsilon(1 + \phi_s)\int^s (1 - \cos\phi)ds.\end{aligned} \tag{33}$$

The linearized phase equation around the zero solution becomes

$$\partial_t \phi = \phi_{ss} + (1+\epsilon)\phi. \tag{34}$$

Expanding ϕ with Fourier modes as $\phi = -\sum a_n(t) \sin ns$, we get

$$\dot{a}_n = (1 + \epsilon - n^2) a_n. \tag{35}$$

Thus, when ϵ is small but finite, the $n = 1$ mode is the sole slow critical mode effective in long-term dynamics, hence it is possible to derive the effective description including only the $n = 1$ mode [15].

Our construction of the nonlocal perturbation in which we introduced a virtual potential circle might seem unusual to some readers. We could have selected any other type of nonlocal perturbation; however, this type is heuristically introduced as a simple example of a possible nonlocal perturbation. It is important to note that the local description given by Eqs. (1) and (2) is structurally unstable. Hence, almost any type of nonlocal perturbation unfolds the neutral stability of Brower's dynamics. Therefore, we conclude that the slow mode equation that will be derived here after is universal within the $\mathcal{O}(\epsilon)$ neighbor of the system constructed under the locality assumption.

Now, we perform singular perturbation to derive the coarse-grained dynamical equation, assuming that ϵ is sufficiently small. Equation (33) is approximated and rewritten as

$$\hat{\ell}_0 \phi = \frac{\partial \phi}{\partial t} - \epsilon\phi + N_2(\phi) + N_3(\phi), \tag{36}$$

where $\hat{\ell}_0$ is the linear operator

$$\hat{\ell}_0 = \frac{\partial^2}{\partial s^2} + 1, \tag{37}$$

N_2 and N_3 are the second and third order nonlinear functions of ϕ given by

$$N_2(\phi) = -\phi\phi_s - \int \phi_s^2 ds, \tag{38}$$

$$N_3(\phi) = -\phi_s \int \phi_s^2 ds. \tag{39}$$

We define the small parameter ε as $\epsilon = R\varepsilon$, with which we give the naïve perturbation series $\phi = \phi_0 + \varepsilon\phi_1 + \varepsilon^2\phi_2 + \cdots$. Further introducing the multiple slow time scales $t = \varepsilon^{-1}\tau + \varepsilon^{-2}\tau_2$, we obtain the perturbation series

$$O(\varepsilon): \ \hat{\ell}_0 \phi_1 = 0, \tag{40}$$

$$O(\varepsilon^2): \hat{\ell}_0 \phi_2 = \frac{\partial \phi_1}{\partial \tau} - R\phi_1 - \phi_1\phi_{1s} - \int^s {\phi_{1s}}^2 ds, \tag{41}$$

$$O(\varepsilon^3): \hat{\ell}_0 \phi_3 = \frac{\partial \phi_1}{\partial \tau_2} + \frac{\partial \phi_2}{\partial \tau} - \phi_{1s} \int^s {\phi_{1s}}^2 ds - \int^s \phi_{1s}\phi_{2s} ds - \phi_1\phi_{2s} - \phi_{1s}\phi_2. \tag{42}$$

The $\mathcal{O}(\varepsilon)$ equation gives the zero eigenvalue function $\phi_1 = -a_1(t)\sin s$. From the solvability condition for the $\mathcal{O}(\varepsilon^2)$ equation, we get the slow mode equation by

$$\frac{da_1}{d\tau} = Ra_1 - a_1^2 + \mathcal{O}(a_1^3), \tag{43}$$

which is the normal-form equation of transcritical bifurcation. Here, we simultaneously consider the centroid velocity in the lowest order approximation. Although we introduced the nonlocal perturbation, the perturbation is $\mathcal{O}(\epsilon)$; hence, the effect of the perturbation on the centroid is significantly less than that of the locality assumption. Thus, it is sufficient to consider Eq. (25) as the lowest order velocity relation. Considering Eq. (25) with Eq. (43), we finally conclude that Eq. (43) is the drift bifurcation equation of a self-propelled interface. We continue with the perturbation analysis until $\mathcal{O}(\varepsilon^3)$ for a more detailed investigation. Solving the $\mathcal{O}(\varepsilon^2)$ equation under the solvability condition, we get

$$\phi_2 = \sum_{n\geq 2} b_n \sin ns, \tag{44}$$

where

$$b_2 = \frac{1}{12}a_1^2, \quad b_n = \frac{(-1)^n}{n(1-n^2)}a_1^2 \quad (n \geq 3). \tag{45}$$

Introducing the obtained ϕ_1, ϕ_2 into the $\mathcal{O}(\varepsilon^3)$ equation, we obtain the higher order solvability condition

$$\frac{da_1}{d\tau_2} = \frac{1}{12}a_1^3. \tag{46}$$

Thus setting $\varepsilon = 1$, we finally get the slow equation of motion

$$\frac{da_1}{d\tau} = Ra_1 - a_1^2 + \frac{1}{12}a_1^3 + \mathcal{O}(a_1^4). \tag{47}$$

We see that the sign of the third order term is positive.

Figure 2 (A) shows the bifurcation diagram of Eq. (47). We see that the complete circle is stable at $R < 0$, but this solution becomes unstable via the transcritical (TC) bifurcation at $R = 0$. Although it is interesting to notice that the stable branch vanishes through the saddle-node (SN) bifurcation occurring at $R = 3$ in the diagram, the solution around $R = 3$ is unrealistic because it has several intersection points. Figure 2 (B) illustrates the several solutions obtained on the stable branch. As shown in Fig. 2 (B)(c), the curve starts to intersect around $R \simeq 2.46$. The solutions above this point should be prohibited, considering the long-range interaction avoiding the intersection. Figure 3 shows an example of the spontaneous drift dynamics of the broken interface obtained numerically by solving Eqs. (25) and (47). We see that the initially circular interface becomes an arc accompanying a spontaneous drift motion. Thus, we conclude that the transcritical drift bifurcation robustly appears with the unfolding of Brower's description of interface.

Finally, we give a brief explanation on the origin of the transcriticality. Our theory is constructed by assuming that the curve has spontaneous curvature, which implies that

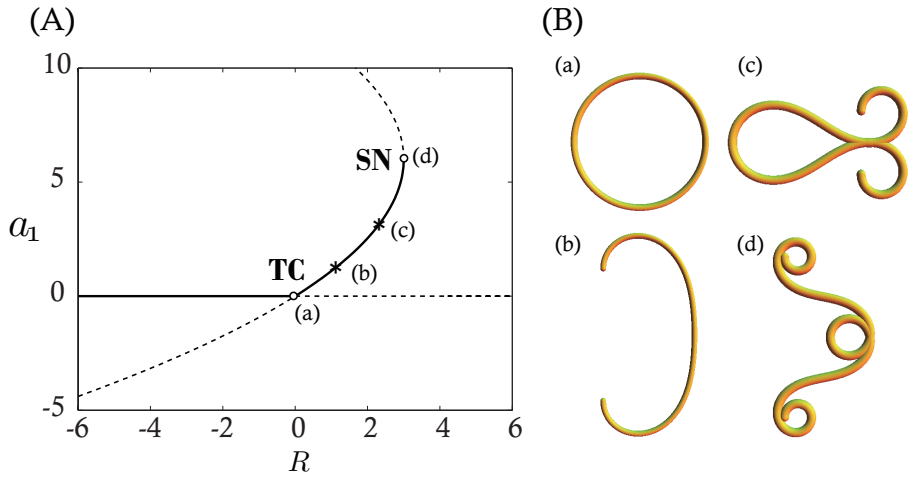

Figure 2. (Colour on-line) (A) Bifurcation diagram of fixed point of broken interface. The bold and dotted lines are the stable and unstable branches respectively. The broken interface creates spontaneous drift via the transcritical (TC) bifurcation at $R = 0$, and the stable branch collapses via the saddle-node bifurcation (SN) at $R = 3.0$. (B) The solutions obtained on the stable branch, in which the values of the parameter are (a) $R = 0$ (b) $R = 0.75$ (c) $R = 2.46$ (d) $R = 3.0$. The curves (b), (c) and (d) move rightward.

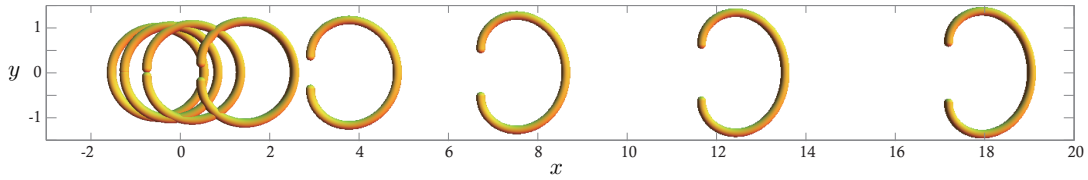

Figure 3. (Colour on-line) Spontaneous drift motion of broken interface. The value of the parameter is set to $R = 0.5$. The initial state is selected to a complete circular shape $a_1 = 0$ and a small perturbation $\delta a_1 = 10^{-4}$ is appended at $t = t_{\rm on}$. The resultant drift motions obtained at $t - t_{\rm on} = 0, 12, 14, 16, 18, 20, 22, 24$ are depicted.

the convex and concave bendings have different effects. With this bending asymmetry, Eq. (32) is not invariant against the operation $\phi \to -\phi$, from which the transcriticality originates. If we assumed the other simple case $U \sim -\kappa$, instead of Eq. (3), the bending symmetry is recovered, hence the drift bifurcation should become supercritical.

4. Discussion

In this letter, we have considered a geometrical model of broken interface and demonstrated that nonlocal force is necessary to describe the universal property of a self-propelled broken interface.

Some readers might be unsatisfied that our theory considers an open interface having two free terminals, while examples of self-propelled objects presented in the introduction should be treated as a domain or a closed circular surface rather than an

open line element in a $2d$ system. However, we consider that our model might be one effective description of the dynamics of a highly deformed self-propelled spot. In order to explain it, we recall the description of a spiral pattern in the $2d$ excitable system. Although the spiral is the $2d$ extended pattern having front and back interfaces, almost all properties of a spiral pattern are explained by the geometrical model of a single interface having a free terminal, except for the properties related to the core [16, 17]. In a similar way, we consider that some properties of moving deformed spot might be also determined by the $1d$ geometry of the open interface. For example, we consider that one of the plausible applications of our model is the deformed spot pattern in the photosensitive BZ reaction with feedback control [11]. The BZ reaction with feedback control is compatible with our theory, because the feedback control is described as the nonlocal effect in the geometrical point of view. For the description of the steady moving spot of BZ reaction, Zykov *et al.* already showed that the shape of a moving domain is determined by the velocity-curvature relationships of front and back pulses in the Fitzhugh-Nagumo reaction-diffusion system [18]. However, under the static approach of Zykov *et al.*, it is difficult to consider the plentiful dynamics of spot patterns. On the other hand, our model is more productive on modifying the nonlocal operator because it includes nonlinear interactions among the various shape modes [19]. This study is in progress and will be presented in future works.

Finally, we discuss the possible applications of this study in biological problems. One such example that can be considered is the description of a fish keratocyte, which is a basic model organism that has investigated for a long time, seeking the mechanisms of cell locomotion [20]. The simple mathematical model of a keratocyte is already proposed [21] in which the cell is represented by two self-propelled elements connected by a spring. In addition to their description, we propose to consider that a keratocyte is a pseudo-line element with nonlocal force because several properties reported for keratocytes seem suitable with our pseudo-line description. For example, analogous to the two geometrically singular points $\mathbf{r}(-\pi)$ and $\mathbf{r}(\pi)$ assumed in our model, keratocytes also have two mechanically singular points called focal adhesion points, where the cell strongly adheres to the substrate [22]. Moreover, it has been pointed out that the geometric nature of a keratocyte is effective in the determination of the cell velocity [23]. The nonlocality assumed in our model can be interpreted as a reduced expression of many slow variables like organelles existing near the interface [20]. It is said that the actin flow has an essential role in self-propelling motion of keratocyte [20], and we conjecture that the vector $V\mathbf{t}$ is related to the fluid flow called "retro-grade flow." The vector $V\mathbf{t}$ is introduced as a multiplier having the dimension of force to sustain the surface shape in our theory. However, several researchers considers that the tangential force cannot be made by the intracellular circumstances (this consideration is called the graded radial extension hypothesis) [24]. Therefore, if we appreciate the radial extension hypothesis, the vector $V\mathbf{t}$ should be interpreted to be something having he dimension of force. We consider that one possible interpretation of $V\mathbf{t}$ is a fluid flow, and, therefore, we are investigating whether the interpretation explains various intracellular

fluid properties. However, we also have troubles to explain the motion of keratocyte; for example, the spontaneous motion of a keratocyte seems subcritical because a transition from the stationary state to locomotion is induced using a finite controlled mechanical stimulus [25]. Subcritical bifurcation is not produced with our present model; therefore, we consider that further modification of our model is necessary to explain the motion of a keratocyte. We believe that the geometrical approach is promising for the more precise description of bio-motility.

Acknowledgments

We acknowledges H. Wada for a lot of helpful comments.

References

[1] Hong Y Blackman N M K Kopp N D Sen A and Velegol D 2007 Chemotaxis of Nonbiological Colloidal Rods Phys. Rev. Lett. 99 178103.
[2] Valadares L F Tao Y-G Zacharia N S Kitaev V Galembeck F Kapral R and Ozin G A 2010 Catalytic Nanomotors: Self-Propelled Sphere Dimers Small 6 565.
[3] Rückner G and Kapral R 2007 Chemically Powered Nanodimers Phys. Rev. Lett. 98 150603.
[4] Gangwal S Cayre O J Bazant M Z and Velev O D 2008 Induced-Charge Electrophoresis of Metallodielectric Particles Phys. Rev. Lett. 100 058302.
[5] Jiang H-R N Yoshinaga and M Sano 2010 Active Motion of a Janus Particle by Self-Thermophoresis in a Defocused Laser Beam Phys. Rev. Lett. 105 268302.
[6] Sumino Y Magome N Hamada T and Yoshikawa K 2005 Self-Running Droplet: Emergence of Regular motion From Nonequilibrium Noise Phys. Rev. Lett. 94 068301.
[7] Sugawara 2009 *Evolutionary Biology - Concept, Modeling, and Application* ed. Pontarotti P. (Berlin: Springer).
[8] Krischer K and Mikhailov A 1994 Bifurcation to Traveling Spots in Reaction-Diffusion Systems Phys. Rev. Lett. 73 3165.
[9] Whitelam S Bretschneider T and Burroughs N J 2009 Transformation from Spots to Waves in a Model of Actin Pattern Formation Phys. Rev. Lett. 102 198103.
[10] Astrov Y A and Purwins H-G 2001 lasma Spots in a gas discharge system: birth, scattering and formation of molecules Physics Letters A 283 349.
[11] Sakurai T Mihaliuk Chirila F and Showalter K 2002 Design and Control of Wave Propagation Patterns in Excitable Media SCIENCE 296 2009.
[12] Brower R C Kessler D A Koplik J and Levine H 1984 Geometrical models of interface evolution Phys. Rev. A 29 1335.
[13] Goldstein R and Langer S 1995 Nonlinear Dynamics of Stiff Polymers Phys. Rev. Lett. 75 1094.
[14] Wiggins S 2003 *Introduction to Applied Nonlinear Dynamical Systems and Chaos* (Berlin: Springer).
[15] Kuramoto Y 1984 *Chemical Oscillations, Waves, and Turbulence* (Berlin: Springer).
[16] Pelcé P and Sun J 1991 Wave front interaction in steadily rotating spirals Physica D 48 353.
[17] Mikhailov A S and Zykov V S 1994 Kinematical theory of spiral waves in excitable media: Comparison with numerical simulations Physica D 70 1.
[18] Zykov V S and Showalter K 2005 Wave front interaction model of stabilized propagating wave segments Phys. Rev. Lett. 94 068302.
[19] Ohta T Ohkuma T and Shitara K 2009 Deformation of a self-propelled domain in an excitable reaction-diffusion system Phys. Rev. E 80 056203.

[20] Keren K. Yam P T Kinkhabwala A Mogilner A and Theriot J A 2009 Intracellular fluid flow in rapidly moving cells Nature Cell Biol. 10 1219.
[21] Barnhart E L Allen G M Julicher F and Theriot J A 2010 Bipedal Locomotion in Crawling Cells Biophys J. 98 933.
[22] Fournier M F Sauser R Ambrosi D Meister J-J and Verkhovsky A B 2010 Force transmission in migrating cells J. Cell Biol. 188 287.
[23] Keren K Pincus Z Allen G M Barnhart E L Marriott G Mogilner A and Theriot J A 2008 Mechanism of shape determination in motile cells Nature 453 475.
[24] Lee J Ishihara A and Jacobson K 1993 How do cells move along surfaces? Trend. cell Biol. 3 166.
[25] Verkhovskey A B Svitkina T M and Borisy G G 1999 Self-polarization and directional motility of cytoplasm Curr. Biol. 9 11.